Midlatitude westerlies, atmospheric CO_2, and climate change during the ice ages

J. R. Toggweiler,[1] Joellen L. Russell,[2,3] and S. R. Carson[1,4]

[1]   An idealized general circulation model is constructed of the ocean's deep circulation and CO_2 system that explains some of the more puzzling features of glacial-interglacial CO_2 cycles, including the tight correlation between atmospheric CO_2 and Antarctic temperatures, the lead of Antarctic temperatures over CO_2 at terminations, and the shift of the ocean's $\delta^{13}C$ minimum from the North Pacific to the Atlantic sector of the Southern Ocean. These changes occur in the model during transitions between on and off states of the southern overturning circulation. We hypothesize that these transitions occur in nature through a positive feedback that involves the midlatitude westerly winds, the mean temperature of the atmosphere, and the overturning of southern deep water. Cold glacial climates seem to have equatorward shifted westerlies, which allow more respired CO_2 to accumulate in the deep ocean. Warm climates like the present have poleward shifted westerlies that flush respired CO_2 out of the deep ocean.

Citation: Toggweiler, J. R., J. L. Russell, and S. R. Carson (2006), Midlatitude westerlies, atmospheric CO_2, and climate change during the ice ages, *Paleoceanography*, *21*, PA2005, doi:10.1029/2005PA001154.

1.   Introduction

[2]   Shortly after *Delmas et al.* [1980] and *Neftel et al.* [1982] discovered that atmospheric CO_2 was lower at the peak of the last ice age, *Broecker* [1982] suggested that the CO_2 reduction had come about through an increase in the ocean's biological activity. He reasoned that a larger flux of sinking organic particles in a more productive glacial ocean would be in balance with a larger CO_2 gradient between the surface ocean and deep ocean. A larger CO_2 gradient would put more CO_2 into the deep ocean and leave less CO_2 for the atmosphere and surface ocean.

[3]   Two aspects of Broecker's hypothesis have endured and have guided most of the ensuing research. The first is the idea that a biogeochemical mechanism lowered the atmospheric pCO_2 by increasing the amount of CO_2 in the deep ocean. The second is the idea that the biogeochemical mechanism responds in some way to subtle changes in the Earth's orbit and spin axis [*Milankovitch*, 1930]. Broecker figured that the orbit and spin axis would operate first on the Northern Hemisphere ice sheets. The ice sheets would then alter the ocean's biological activity through their impact on sea level.

[4]   It has been clear for some time that the rise in CO_2 at glacial terminations occurs before changes in global ice

volume [*Shackleton and Pisias*, 1985; *Sowers et al.*, 1991]. This means that the effect of the orbital forcing on CO_2 is not being mediated through the ice sheets and it implies that the orbital forcing is somehow operating more directly on the ocean's biogeochemistry [*Shackleton*, 2000]. It is hard to imagine, however, why the biogeochemistry should be so sensitive to this kind of forcing.

[5]   Here we lay out a different approach. We call for a positive feedback that shoots atmospheric CO_2 from glacial extremes to interglacial extremes and back again. The proposed feedback is internal to the climate system. An interaction between the ocean's circulation, atmospheric winds, and atmospheric CO_2 pushes the atmospheric pCO_2 up and down, not the biogeochemistry or the orbital forcing.

[6]   Organic particles sinking out of the upper ocean leave the residual CO_2 in the upper ocean and atmosphere enriched in $\delta^{13}C$. When the organic particles are respired at depth they make the CO_2 in the interior depleted in $\delta^{13}C$. Past changes in respired CO_2 can be reconstructed from this relationship. Extensive mapping of the $\delta^{13}C$ distribution at the Last Glacial Maximum (LGM) shows that the ocean did indeed retain more respired CO_2 à la *Broecker* [1982] but the CO_2 accumulated only near the bottom of the ocean [*Duplessey et al.*, 1988; *Herguera et al.*, 1992; *Sarnthein et al.*, 1994; *Matsumoto and Lynch-Stieglitz*, 1999; *Mackensen et al.*, 2001].

[7]   Figure 1 shows the difference in $\delta^{13}C$ between the modern ocean and the LGM along a transect of cores through the eastern Atlantic. The deep South Atlantic was particularly depleted in $\delta^{13}C$ and held much more respired CO_2 than it does today. The upper half of the Atlantic was enriched in $\delta^{13}C$ and had less CO_2. The contour of zero $\delta^{13}C$ difference, the red contour in Figure 1, divides the deep Atlantic into a part that accumulated respired CO_2 (below)

---

[1]Geophysical Fluid Dynamics Laboratory, NOAA, Princeton, New Jersey, USA.

[2]Atmospheric and Oceanic Sciences Program, Princeton University, Princeton, New Jersey, USA.

[3]Now at Department of Geosciences, University of Arizon, Tucson, Arizona, USA.

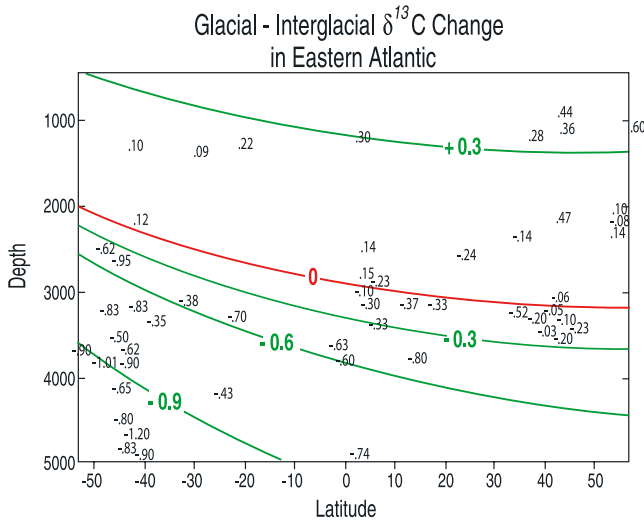[4]Now at John Witherspoon Middle School, Princeton, New Jersey, USA.

Figure 1. Change in $\delta^{13}C$ between the modern and glacial Atlantic due to the buildup of respired CO_2 at depth (units per mil). The red (bold) contour of zero $\delta^{13}C$ difference in the center divides the Atlantic into a part that accumulated respired CO_2 (below) from a part that lost CO_2 (above). Figure 1 was constructed by subtracting the $\delta^{13}C$ of the water overlying 56 sediment cores in the eastern Atlantic from the $\delta^{13}C$ of benthic foraminifera of glacial age (after *Duplessey et al.* [1988], *Kroopnick* [1985], and *Boyle* [1992], with additional data from *Curry et al.* [1988], *Flower et al.* [2000], *Hodell et al.* [2003], and *Mackensen et al.* [2001]). A value of 0.3‰ was added to the difference to remove the effect of isotopically light terrestrial carbon that invaded the ocean during the last glacial period.

from a part that lost CO_2 (above). The mean depth of the red contour is about 2500 m.

[8] *Hodell et al.* [2003] constructed a time series of $\delta^{13}C$ changes with depth from a series of cores between 40° and 45°S in the South Atlantic. Their results, reproduced here as Figure 2, show that there was a large accumulation of respired CO_2 below 2500 m during every glacial stage ($\delta^{18}O$ stages 2–4, 6, 8, 10, 12, and 14). Roughly the same amount of respired CO_2 built up during each cold period. There is relatively little buildup of respired CO_2 during the present interglacial (stage 1) and earlier interglacials (stages 5, 9, 11, and 13).

[9] The ocean below 2500 m comes into contact with the atmosphere mainly around Antarctica. Hence the most likely explanation for the glacial $\delta^{13}C$ pattern in Figures 1 and 2 is a change in circulation or ventilation that isolates the water below 2500 m and blocks the evasion of respired CO_2 back up to the atmosphere [*Toggweiler*, 1999].

[10] The process that exposes the deep water below 2500 m to the atmosphere today is the upwelling around Antarctica that is forced by the westerly winds over the Antarctic Circumpolar Current (ACC) [*Wyrtki*, 1961; *Gordon*, 1971; *Toggweiler and Samuels*, 1993]. Weaker westerlies that induce less upwelling should reduce the ventilation of the deep water below 2500 m; stronger westerlies should produce more upwelling and more ventilation.

[11] The position of the strongest westerlies in relation to the ACC is a critical factor. When the strongest westerlies are relatively close to Antarctica and are aligned with the ACC they give rise to a larger divergence and more upwelling of deep water from the interior. If they are far away from Antarctica and are poorly aligned with the ACC they would bring less deep water up to the surface. J. L. Russell et al. (The Southern Hemisphere westerlies in a warming world: Propping open the door to the deep ocean, submitted to *Journal of Climate*, 2005) have used a state-of-the-art coupled model to show that a 3°–4° poleward shift in the mean position of the westerlies significantly increases the ventilation of the deep water around Antarctica.

[12] Here we posit that the glacial westerlies were so far equatorward of their present position that they did not upwell any deep water next to Antarctica. With no upwelling and no ventilation, there was a big buildup of respired CO_2 below 2500 m. Our specific hypothesis is that changes in the position of the westerlies take place through a positive feedback in which a poleward shift in the westerlies gives rise to more upwelling and more CO_2 in the atmosphere; more CO_2 in the atmosphere gives rise, in turn, to a larger poleward shift in the westerlies, still more upwelling, and still more CO_2.

[13] A key aspect of the feedback is demonstrated here in an idealized general circulation model that includes the full oceanic CO_2 system. The model solution evolves in time and produces realistic glacial-interglacial CO_2 cycles. Our presentation begins with a cartoon description of the ocean's circulation and biogeochemistry (section 2) and a statement of our hypothesis regarding the feedback (section 3). The model and our results are presented in section 4.

[14] A follow-up paper (J. R. Toggweiler, manuscript in preparation, 2006) uses a box model to show how individual feedback events are spaced out in time to produce the
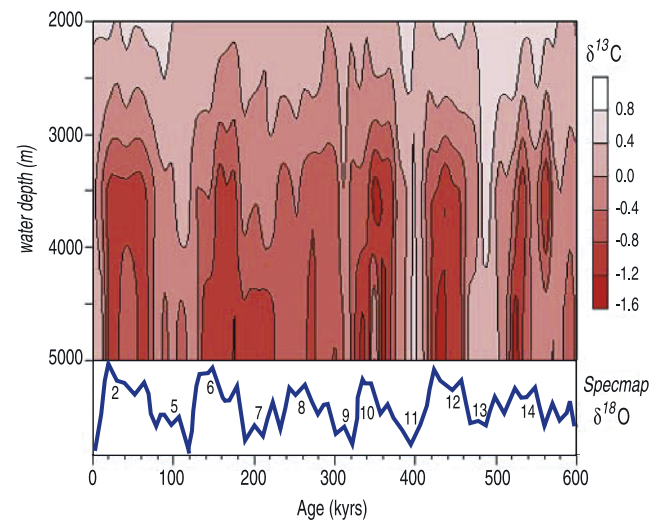

Figure 2. Change in $\delta^{13}C$ over the last 600,000 years in a sequence of cores from different depths between 40° and 45°S in the South Atlantic. The Specmap $\delta^{18}O$ record (blue line at the bottom) is shown for reference. Reproduced with permission from *Hodell et al.* [2003].

100,000-year cycles seen in Figure 2 and in the Vostok CO_2 record [*Petit et al.*, 1999]. Section 5.4 previews the follow-up paper.

2. Basic Elements

[15] The critical elements of the ocean's deep circulation and carbon cycle are illustrated with the help of the cartoon in Figure 3. As depicted here, the deep ocean has northern and southern overturning circulations that occupy distinct domains in the interior. The mid depth northern domain is the domain of North Atlantic Deep Water (NADW). Its circulation is colored red in Figure 3. The southern domain is the domain of the deep and bottom water formed around Antarctica. Its circulation is colored blue. The divide in Figure 1 falls along the boundary between the northern and southern circulations. Respired CO_2 accumulates during glacial periods in the deep blue domain.

[16] Northern and southern water in the modern ocean mixes together in the interior to form the water mass known as Circumpolar Deep Water (CDW), which comes up to the surface along the southern flank of the ACC. The upwelling of CDW is forced to a large extent by the divergence in the surface flow forced by the midlatitude westerlies [*Gordon*, 1971; *Toggweiler and Samuels*, 1993, 1995]. The box labeled "DP/ACC" in Figure 3 depicts the upwelling zone.

[17] The northern component of upwelled CDW is driven northward in the surface Ekman layer and then makes a long traverse through the thermoclines of the Indian, Pacific, and Atlantic before reaching its zone of sinking in the North Atlantic [*Gnanadesikan*, 1999]. It is exposed to biological activity along this route. Organisms strip the nitrate and phosphate from the upwelled water and produce organic particles that fall into the deep ocean, as indicated by the brown squiggly lines.

[18] The southern component, on the other hand, sinks almost immediately back into the deep ocean [*Gordon*, 1971]. As such, it is exposed to very little biological activity and it gives rise to few organic particles. Sinking southern water in the real ocean is observed to have essentially the same amount of phosphate as upwelled CDW [*Foster and Carmack*, 1976; *Weiss et al.*, 1979].

[19] The northern red circulation is the source of virtually all the organic particles that fall into the deep ocean, but these "northern" particles are respired in both the red and blue domains. Respiration of the particles elevates the pCO_2 of both water types above the pCO_2 in the atmosphere. The respired CO_2 is thus primed to escape when CDW comes up to the surface.

[20] When the southern component comes up to the surface its pCO_2 remains high because of the limited biological activity in the blue zone next to Antarctica. Its respired CO_2 escapes to the atmosphere fairly easily. The situation with the northern component is different because its pCO_2 is drawn down as its nutrients are utilized. The respired CO_2 in upwelled northern water ends up back down in the deep ocean instead of the atmosphere.

[21] If the blue circulation is weak while the red circulation remains active, the escape of respired CO_2 back up to the atmosphere will be impeded. Respired CO_2 will build up
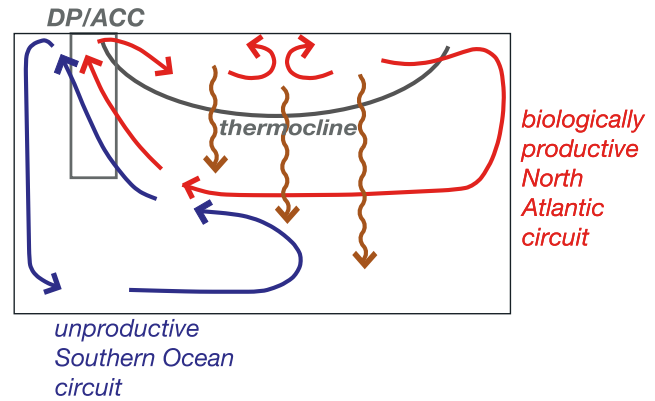

Figure 3. Relationship between the ocean's deep circulation and its pool of respired CO_2. This cartoon reduces the ocean's overturning to two components: a northern (red, solid black) circulation and a southern (blue, dashed grey) circulation. Respired CO_2 accumulates during glacial periods in the deep southern domain because the southern (blue) circulation was inactive or very weak. The box labeled "DP/ACC" depicts the ocean's main upwelling zone along the southern flank of the Antarctic Circumpolar Current in the latitude band of Drake Passage.

in the stagnant blue domain as the CO_2 contents of the atmosphere and upper ocean fall. This is our scenario for the glacial ocean.

[22] Basically, the process that puts respired CO_2 into the blue zone below 2500 m, the production of particles by the northern red circulation, is assumed to be independent of the process that brings the respired CO_2 from the blue zone back up to the surface, the southern blue circulation. This independence gives the climate system the potential to shift a large quantity of CO_2 between the atmosphere and deep ocean.

3. Role of the Westerlies

[23] The results in Figure 2 suggest that the blue circulation in Figure 3 has been either on or off for the last 600,000 years. It does not seem to remain in an intermediate state for very long. Our hypothesis is that this on/off behavior is due to a positive feedback that pushes the Southern Ocean toward a state with active ventilation or one with no ventilation. The feedback comes about through a link between the midlatitude westerlies, the upwelling of southern deep water around Antarctica, and atmospheric CO_2.

[24] The westerlies in the Southern Hemisphere today are very strong and are fairly close to Antarctica. This makes the divergence in the surface flow around Antarctica fairly large. As such, the westerlies draw up a large volume of deep water close to Antarctica where it is rather easily modified into new deep water. The strongest westerlies at the LGM seem to have been some $7°-10°$ north of their present position (e.g., *Moreno et al.* [1999] and many others, see section 5). At this distance from Antarctica, the divergence would have been substantially weaker and less effective.

[25] The westerlies shifted poleward toward their modern position as the climate warmed following the LGM. Details about the shift are sketchy (again, see section 5), but the empirical fact that a shift occurred is strongly supported by observations showing that the surface westerlies have been shifting poleward over the last 40 years [*Hurrell and van Loon*, 1994; *Shindell and Schmidt*, 2004] largely in response to the warming induced by anthropogenic CO$_2$. Thus there seems to be a general relationship between the position of the westerlies and the climate: warm climates like the present tend to have poleward shifted westerlies; cold climates like the one at the LGM have equatorward shifted westerlies [*Williams and Bryan*, 2006].

[26] This tendency of the westerlies and its relationship to the blue circulation is a recipe for a positive feedback (Figure 4). Imagine a warming trend that causes the westerlies to shift slightly poleward. The shift causes more deep water to come to the surface close to Antarctica and flushes more respired CO$_2$ out to the atmosphere. Higher CO$_2$ leads to warmer temperatures and a larger poleward shift in the westerlies. This leads to an even stronger blue circulation, more CO$_2$, warmer temperatures, etc.

[27] The feedback should also work in the other direction. A cooling trend that leads to an equatorward shift in the westerlies weakens the blue circulation and causes more respiration CO$_2$ to accumulate in the deep ocean. Lower CO$_2$ leads to cooler temperatures and an additional equatorward shift in the westerlies. This leads to lower CO$_2$, still cooler temperatures, etc.

[28] The proposed feedback is bounded because the deep ocean can hold and give up only so much respired CO$_2$. The feedback in the warm direction stops when an active blue circulation has flushed most of the respired CO$_2$ out of the blue domain. The feedback in the cold direction stops when a dead blue circulation allows the blue domain to retain the maximum amount of respired CO$_2$.

4. CO$_2$ Response to the Westerlies

4.1. Overview

[29] Here we describe a three-dimensional ocean circulation model in which a simple variation of the wind-forcing around Antarctica generates many of the CO$_2$ changes associated with glacial-interglacial cycles. The ocean model, in this case, is coupled to a simple atmospheric model, and the coupled solution evolves with time.

[30] The circulation in the model looks very much like the cartoon in Figure 3. Weaker and stronger westerlies over the Southern Ocean turn the blue circulation off and on and cause respired CO$_2$ to either build up or vent from the ocean below 2500 m, as in Figures 1 and 2. Air temperatures over "Antarctica" rise and fall along with the atmospheric pCO$_2$, as seen in the ice core records of *Petit et al.* [1999]. The rise in atmospheric CO$_2$ lags behind the rise in Antarctic temperatures, as noted by *Fischer et al.* [1999] and *Caillon et al.* [2003]. The ocean model also shifts its highest concentrations of respired CO$_2$ from a glacial position in the Atlantic sector of the Southern Ocean around to its modern position in the North Pacific.
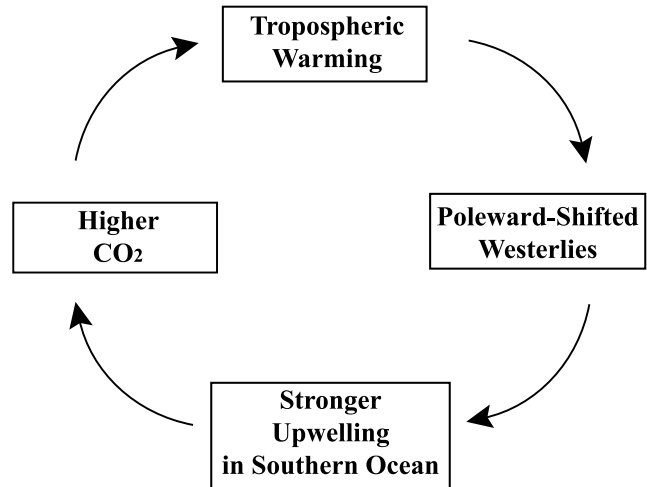

Figure 4. Proposed feedback loop that propels transitions between warm and cold states of the climate system.

[31] The coupling in the model is limited. The ocean and atmosphere are thermally coupled only; the winds must be specified. The blue circulation switches on and off but not through the positive feedback and the shift in the westerlies in Figure 4.

4.2. Model Description

[32] The model used in this paper is based on the Geophysical Fluid Dynamics Laboratory's Modular Ocean Model version 3 (MOM3) (R. C. Pacanowski and S. Griffies, MOM 3. 0 manual, 2000, available at www.gfdl.noaa.gov/oceanic.html). It is built on a 4° grid with 12 vertical levels and has a very simplified distribution of continents [after *Toggweiler and Bjornsson*, 2000]. It has two ocean basins, a long narrow "Atlantic" and a wider shorter "Pacific," which are connected by a circumpolar channel in the south (Figure 5a). The narrow Atlantic basin is shown in the center of Figure 5. Land is limited to two slender meridional barriers, which separate the two basins, and two Antarctica-like polar islands that cover the north and south poles.

[33] Vertical mixing varies with depth [after *Bryan and Lewis*, 1979] from 0.15 cm^2 s^{-1} in the upper kilometer to 1.3 cm^2 s^{-1} near the bottom. The model includes the Gent-McWilliams (GM) parameterization for tracer mixing as implemented for MOM by *Griffies* [1998]. The coefficients governing GM thickness mixing and diffusion along isopycnals have both been set to 0.6×10^7 cm^2 s^{-1}. The model uses the flux-corrected transport (FCT) scheme in MOM3 to advect tracers.

[34] The ocean model is thermally coupled to a two-dimensional energy balance model (EBM) of the atmosphere (written for MOM by I. Held), which is forced by a steady, annually averaged input of short-wave radiation. Atmospheric temperatures are a function of the local short-wave input, long-wave radiation to space (a function of the local temperature), heat exchange with the ocean, and diffusion. The EBM in this case has the same x,y grid as the ocean model.
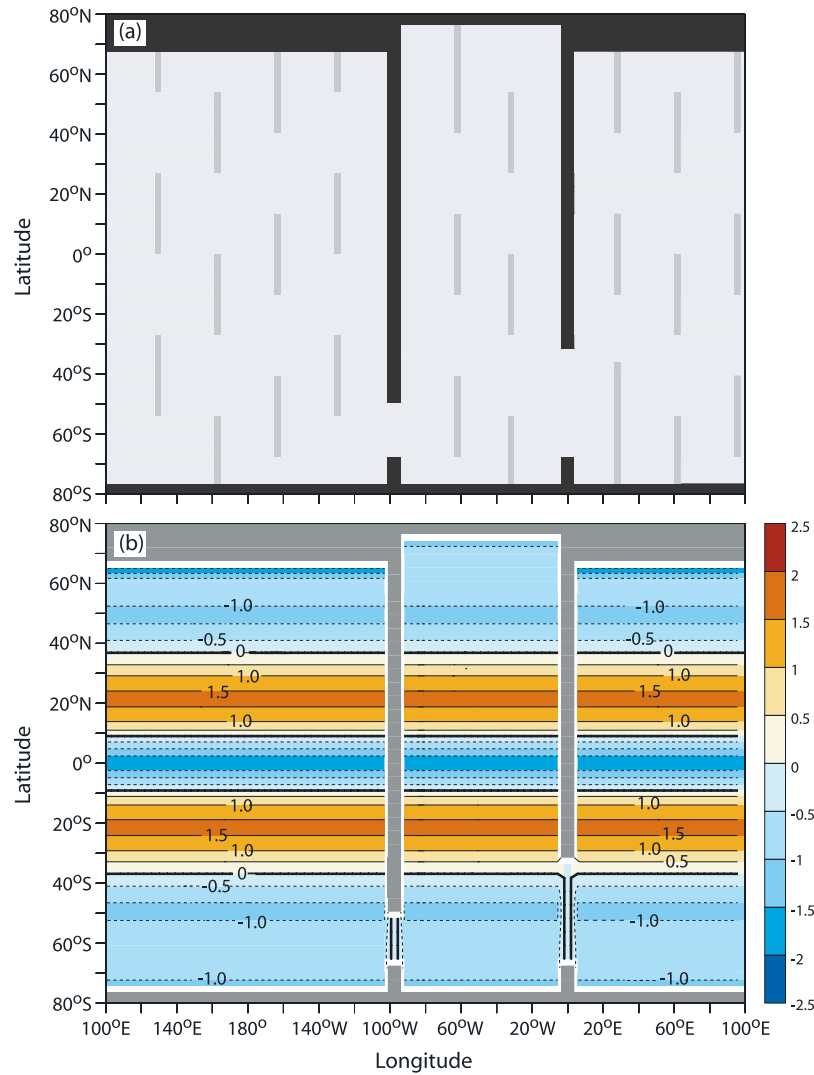
Figure 5. (a) Configuration of land in the three-dimensional ocean model. Two polar islands (the strips of land along the top and bottom) cover each pole out to 76° latitude. The northern polar island extends slightly farther south in the Pacific sector. The ocean basins are flat at the bottom except for a series of north-south trending ridge segments that extend up to 2750 m and are distributed uniformly throughout the domain [after *Toggweiler and Bjornsson*, 2000]. (b) Distribution of the freshwater input used to force salinity in the model. The freshwater input is uniform in the zonal direction and symmetric about the equator. Locations with a net freshwater input to the ocean are colored blue. Locations with net evaporative losses are colored orange. No freshwater falls on the north-south barriers or on the ocean in these longitude bands. Freshwater falling on the polar islands runs off radially into adjacent ocean grid cells (units m/yr).

[35] Salinity is forced by a latitudinally varying field of freshwater fluxes taken from the spin up of the GFDL R30 coupled model [*Knutson and Manabe*, 1998]. The R30 fluxes were averaged around latitude circles and then averaged between the hemispheres to create a flux field that is symmetric about the equator (Figure 5b). There is an excess of precipitation over evaporation at the equator and poleward of 40° in each hemisphere and an excess of evaporation over precipitation between 10° and 40°. The excess precipitation next to the polar islands leads to the formation of low-salinity surface layers that surround

the polar islands. No restoring is employed for either salinity or temperature. There is no provision in the model for freezing or the formation of sea ice.

[36] The basic wind stress field applied to the model is adapted from *Hellerman and Rosenstein* [1983]. It is zonally averaged, like the salinity forcing, to be symmetric about the equator. The stresses south of 30°S are then multiplied by factors of 0.5x, 1.0x, 1.5x, 2.0x, and 3.0x, as given by *Toggweiler and Samuels* [1995], to systematically strengthen the Ekman divergence and the deep upwelling around the south polar island (Figure 6). The
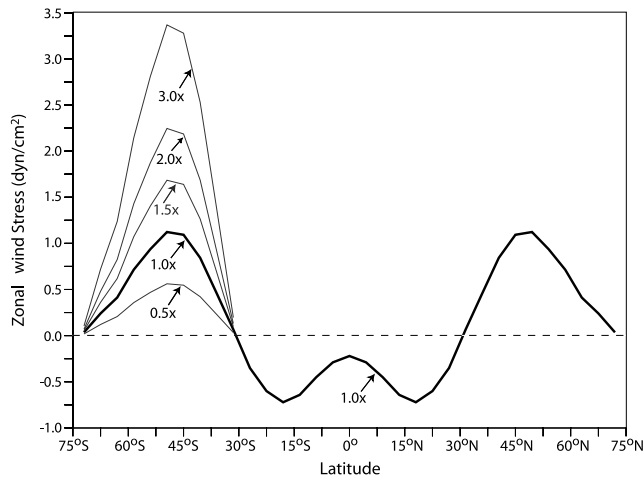
Figure 6. Latitudinal distribution of the wind stress patterns used to force the model. The basic stress pattern, 1.0x, is zonally uniform and symmetric about the equator but is modified so that the stress on the ocean south of 30°S is scaled by factors of 0.5x, 1.5x, 2.0x, and 3.0x. No meridional stress is applied.

distribution of the wind stress field about its latitudinal peak is not altered. The salinity and wind stress fields are held constant with time for each run of the model.

[37] The CO_2 system in the model follows the Biotic-HOWTO protocol from Phase 2 of the Ocean Carbon Model Intercomparison Project (OCMIP-2) (available at http://www.ipsl.jussieu.fr/OCMIP/). It includes tracer fields for temperature salinity, PO_4, O_2, alkalinity, Total CO_2, and Total $^{13}CO_2$. The production of sinking particles is simulated in the model by restoring the surface PO_4 concentrations in each row of ocean grid points toward a fixed latitudinally varying field of surface PO_4 concentrations that is taken from observations. This means that the production of sinking particles is fixed in space and is more or less constant with time. Gas exchange is parameterized by a uniform piston velocity of 3 m/d. The atmosphere is treated as a single well-mixed box with respect to CO_2 and $\delta^{13}C$. The pCO_2 of the atmosphere does not influence the temperature or the radiation balance in the EBM.

4.3. Model Results

4.3.1. Model's 4000-Year Oscillation

[38] When relatively weak winds are applied south of 30°S (0.5x or 1.0x), deepwater formation in the model occurs only in the North Atlantic. The model has a northern red circulation, but no southern blue circulation, and the atmospheric pCO_2 is low. With 2.0x winds, deepwater formation occurs in the south as well. The blue circulation operates along with the red and the pCO_2 is high. With 3.0x winds, deep water formation occurs in the northern Pacific as well. Basically, the wind forcing south of 30°S destabilizes the low-salinity surface layers that form around the two polar islands. Stronger winds cause the polar surface layers to break down one by one. Deepwater formation commences with the breakdown of each fresh surface layer.

[39] If the wind forcing south of 30°S is reduced to 1.5x and held steady at this level, the fresh surface layer around the south polar island begins to re-form and break down on its own. The southern blue circulation then switches on and off with a repeat time of 4000 years. The oscillation is due to changes in the temperature of the deep ocean that stabilize and destabilize the fresh layer around the south polar island.

[40] The blue water forming next to the south polar island is about 3°C colder than the red water forming in the north. The deep ocean warms when the fresh layer is intact and cold blue water is not being added to the deep ocean. When the deep ocean warms to a certain point, the fresh layer breaks down and the blue circulation starts up. When the deep ocean cools the fresh layer re-forms and the blue circulation switches off, etc.

[41] Ocean modelers will recognize the switching on of the southern blue circulation during these transitions as a Southern Hemisphere version of one of the "flushes" described by *Weaver and Sarachik* [1991]. This kind of cycle would never exist in nature because the forcing is never this steady. It is useful here as a convenient "hands off" way of demonstrating how atmospheric CO_2 and the ocean's CO_2 and $\delta^{13}C$ distributions evolve in time in response to changes in the blue circulation.

[42] Figure 7 gives two snapshots of the surface salinity distribution in the 1.5x model, one when the southern blue circulation is active (top) and one when it is inactive (bottom). A fresh layer is present around the south polar island at both times, but it is relatively thin and weak when the blue circulation is active, as seen in Figure 7 top panel. When the blue circulation is inactive in Figure 7 bottom panel, the fresh layer around the south polar island is similar to the fresh layer in the North Pacific.

[43] One convective center continues to operate just east of 180° longitude in the bottom panel. Convection in this one area keeps the deep water in the deep blue domain slightly colder and denser than the water in the red domain. The area of this convective center is so small that it does not enable much venting of CO_2 to the atmosphere.

4.3.2. Atmospheric CO₂ and Antarctic Air Temperatures

[44] The ice core records from Antarctica show a striking temporal correlation between atmospheric CO_2 and the air temperatures over Antarctica [*Petit et al.*, 1999; *Cuffey and Vimeux*, 2001] in which Antarctic temperatures and atmospheric CO_2 rise rather abruptly during each of the last four terminations. A detailed examination of these records shows that Antarctic air temperatures rise several hundred years ahead of atmospheric CO_2 at each termination [*Fischer et al.*, 1999; *Caillon et al.*, 2003].

[45] *Caillon et al.* [2003] give the temperature lead a causal significance. They attribute the temperature increase to the orbital forcing and see temperature as a forcing factor for the CO_2 increase that follows. Here Antarctic air temperatures and atmospheric CO_2 rise and fall as part of a single process. A CO_2 lag is an intrinsic feature. We see the feedback as the cause. The temperature lead is not a significant factor for CO_2.
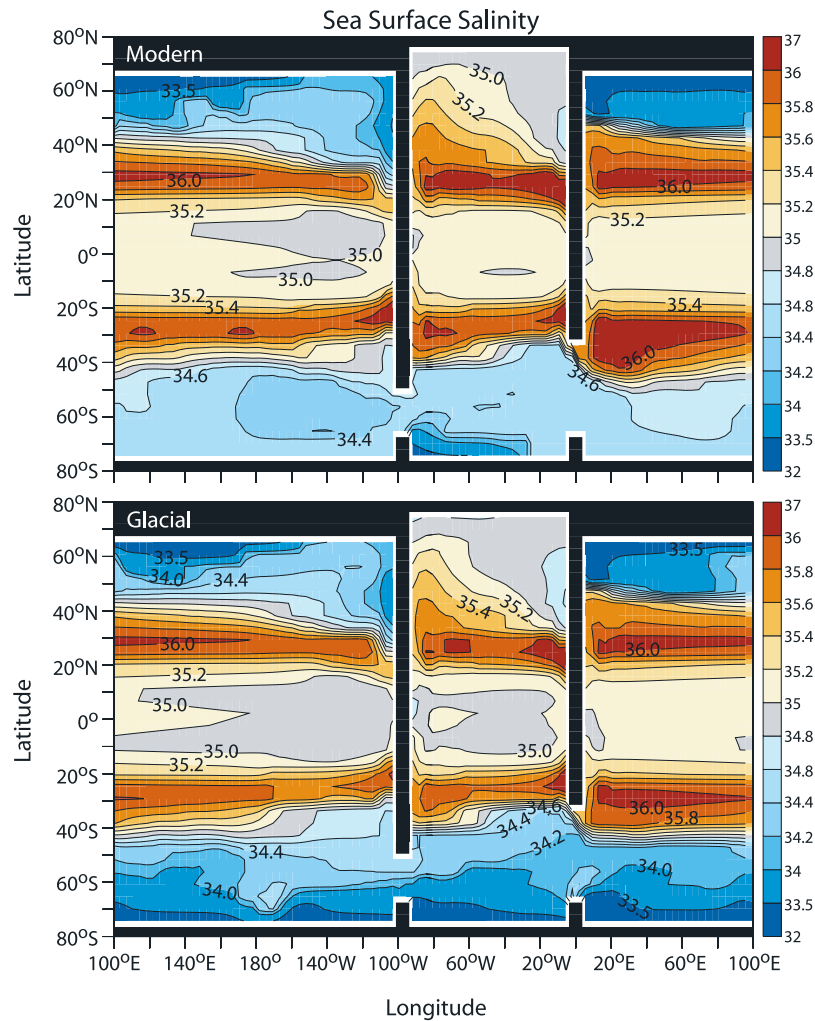
Figure 7. Sea surface salinities with the fresh layer around the South Polar island (top) broken down and (bottom) intact in the 1.5x model. Surface salinities stay close to 35 practical salinity units in the North Atlantic, as the red circulation remains active throughout the run.

[46] Figure 8 shows a pair of time histories for the atmospheric pCO_2 and Antarctic air temperatures from a 12,000-year run of the 1.5x model with steady winds. The "air temperature" in this case is the average air temperature from the first row of atmospheric grid cells over the south polar island at 78°S. The model run starts up at year 0 at the beginning of a warm "interglacial." The southern blue circulation is active and the atmospheric pCO_2 is high. The initial warm period is followed by a cold "glacial" period with a low pCO_2 that begins when the blue circulation switches off. The atmospheric pCO_2 is a bit higher in the first cycle because the CO_2 system in the model is still drifting from its initial conditions.

[47] Three cycles follow. The upper and lower limits of atmospheric CO_2 are about the same in each cycle. This is a consequence of the fact that the deep blue domain has well-defined limits on the size of its pool of respired CO_2. The pool reaches its upper limit, and atmospheric CO_2 reaches its lower limit, when the blue circulation is off. The internal

pool approaches its lower limit, and atmospheric CO_2 reaches its upper limit, when the blue circulation is on and is comparable in strength to the red.

[48] Both time histories are characterized by "terminations" every 4000 years followed by gradual declines back to a cold, low-CO_2 state. These terminations mark times when the fresh layer around the south polar island breaks down and the blue circulation restarts. Air temperatures rise by 4°–5°C. The atmospheric pCO_2 rises by 35 ppm. The rise in the air temperature during one of these terminations leads the rise in CO_2 by about 100 years.

[49] Basically, the upwelling around Antarctica brings warm Circumpolar Deep Water to the surface along with respired CO_2. Thus a strengthening circulation warms the air above Antarctica and releases CO_2 to the atmosphere at the same time. The escape of respired CO_2 from the deep ocean is delayed with respect to heat by the relatively slow rate of gas exchange for CO_2. Gas exchange limits the amount of CO_2 that can escape during each cycle of the blue
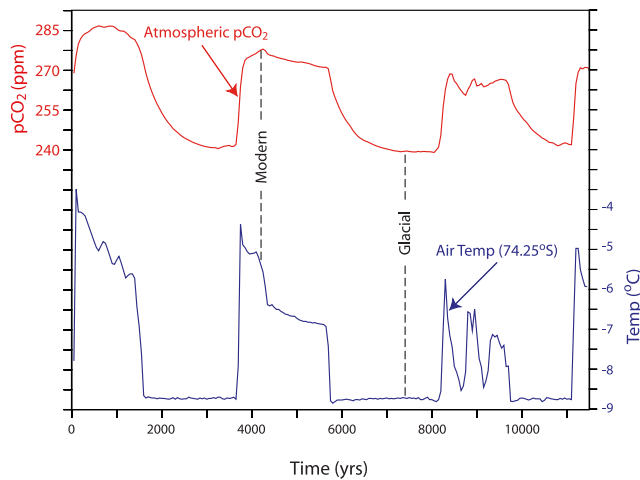
Figure 8. Temporal variation of atmospheric CO_2 and Antarctic air temperature from a 12,000-year run of the 1.5x model. See text for details. Two time slices "Modern" and "Glacial" are marked in Figure 8 and are used in Figures 7, 9, and 10.

water up to the surface. Temperatures also fall more quickly than atmospheric CO_2 during the cooling phase.

[50] The CO_2 variations in Figure 8 have a fairly small range, between 240 and 275 ppm, which is about 40% of the observed range. The 100-year lag in atmospheric CO_2 behind the air temperature over the south polar island is also considerably shorter than the observed lag, $\sim$800 years [*Caillon et al.*, 2003]. However, the present model simulates only one aspect of the CO_2 response to a change in southern ventilation, the so-called "direct effect." There is also an "indirect effect" due to $CaCO_3$ compensation [*Broecker and Peng*, 1987] that is not included in the model. The indirect effect doubles the CO_2 amplitude and extends the CO_2 lag with respect to temperature. The magnitude of the indirect effect is easy to estimate.

[51] *Toggweiler* [1999] developed a box model which distinguishes northern and southern deep water in its deep interior. The model was designed so that the buildup of respired CO_2 during glacial periods would be confined to the lower half of the deep ocean, as seen in Figures 1 and 2. This sort of confinement reduces the direct effect and increases the indirect effect.

[52] Basically the CO_2 concentration in the lower deep box of the *Toggweiler* [1999] model increases twice as much as it does in a similar model with an undifferentiated deep ocean. The higher CO_2 concentration in the lower deep box doubles the CO_2 gradient across the model's Antarctic surface box and makes it harder for the model to suppress the venting of respired CO_2 up to the atmosphere. This makes the direct effect smaller.

[53] The higher CO_2 concentration also doubles the reduction of the $CO_3^=$ concentration in the lower deep box in relation to an undifferentiated deep ocean. A lower $CO_3^=$ concentration at these depths would disrupt the burial of $CaCO_3$ and lead to a more alkaline ocean [*Boyle*, 1988], the indirect effect. The impact of the indirect effect on atmo-

spheric CO_2 is proportional to the $CO_3^=$ deficit. When the buildup of respired CO_2 is confined to the lower half of the ocean à la *Toggweiler* [1999] it produces a large $CO_3^=$ deficit that doubles the direct response to a change in southern ventilation.

[54] The pCO_2 increase due to the indirect effect takes place over some 5000 years [*Broecker and Peng*, 1987]. Thus the combination of an abrupt CO_2 increase from the direct effect (with a 100-year lag behind Antarctic temperatures) and a slow increase from the indirect effect (spread out over 5000 years) could easily create a CO_2 lag that is more like the 800-year lag in the observations.

[55] The present model is also missing another important effect that would boost its pCO_2 response. Air temperatures in the present model do not respond to changes in the atmospheric pCO_2. Interactive air temperatures would have warmed the ocean when the pCO_2 rises and would have led to a further pCO_2 increase. A model with a realistic temperature response should have pCO_2 variations that are about 25 ppm larger than one without [*Toggweiler*, 1999; *Stephens and Keeling*, 2000]. Hence a more complete model with the three processes operating together (on and off southern ventilation, $CaCO_3$ compensation, and warmer and colder temperatures) would have a pCO_2 range of 90 ppm or more, in relation to the 35-ppm range simulated here.

4.3.3. Oceanic TCO_2 and $\delta^{13}C$

[56] Figure 9 shows the change in total CO_2 (TCO_2) in the model's Pacific basin between the model's interglacial and glacial states. The top panel shows the TCO_2 distribution at the peak of the second high-CO_2 interval in Figure 8, the time marked "Modern." The southern blue circulation is on and is efficiently flushing respired CO_2 out of the ocean below 2500 m. The TCO_2 in the North Pacific has a broad maximum at mid depth that is just above the ventilated zone. The TCO_2 maximum in the top panel clearly resembles the TCO_2 maximum in the modern North Pacific.

[57] The middle panel of Figure 9 shows the TCO_2 distribution during the second low-CO_2 interval, the time marked "Glacial" in Figure 8. The results from this time period are quite different. The southern blue circulation is off and is not flushing respired CO_2 from the depths below 2500 m. As a result, the highest TCO_2 concentrations are found along the bottom.

[58] The bottom panel of Figure 9 shows the difference in TCO_2 between the two time slices. The upper ocean above 2500 m has about 50 μmol/kg less CO_2 on average during the low-CO_2 interval. The atmospheric pCO_2 is low because the water in the upper half of the ocean has less CO_2. Deep water below 2500 m has about 50 μmol/kg more CO_2. The line of zero TCO_2 difference passes right through the middle depths of the ocean like the red contour in Figure 1.

[59] The mean TCO_2 concentration at 3500 m, the mean depth of most of the ocean's $CaCO_3$ sediments, is 30–40 μmol/kg higher in Figure 9 middle panel. This result is in good agreement with the *Toggweiler* [1999] box model. TCO_2 concentrations next to the south polar island are especially high during the glacial time slice. The difference plot shows that the water just below the fresh surface layer has 150 μmol/kg more CO_2!
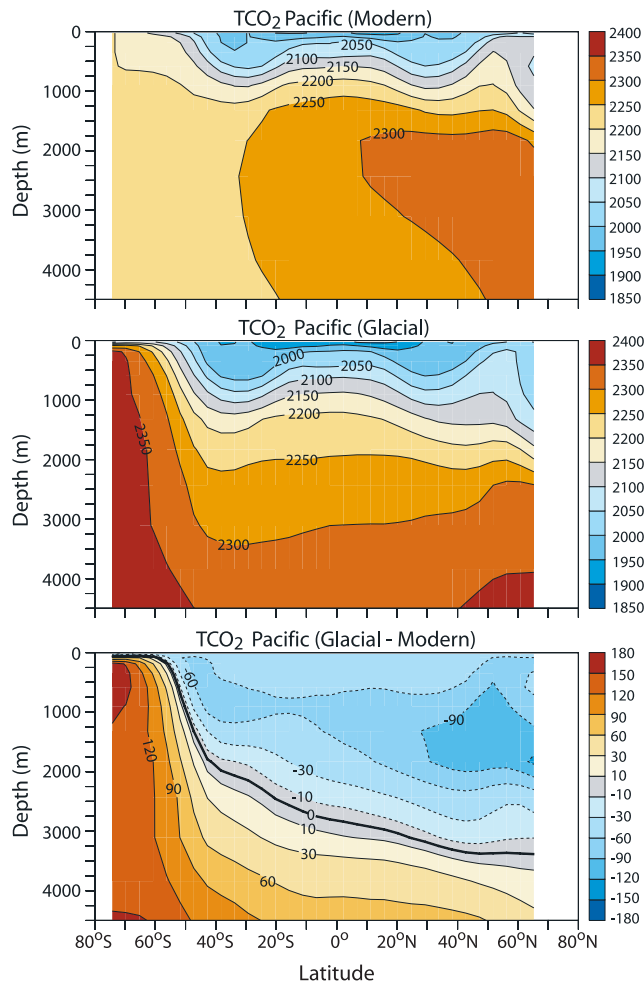
Figure 9. (top) Distribution of total CO₂ (TCO₂) in the Pacific during the time slice marked "Modern" in Figure 8. (middle) Total CO₂ in the Pacific during the "Glacial" time slice in Figure 8. (bottom) Difference in TCO₂ between the two time periods. Units are μmol/kg. Respired CO₂ builds up near the bottom of the ocean when the southern blue circulation switches off. The buildup leads to a CO₂ shift from the atmosphere and the upper half of the ocean into the lower half of the ocean.

[60] The TCO₂ maximum in the top panel of Figure 9 is also a minimum in δ¹³C. The modern δ¹³C minimum is found in the North Pacific because the North Pacific is the most isolated part of the ocean with respect to the sources of new deep water in the North Atlantic and Southern Ocean. The equivalent water type in the glacial ocean was displaced all the way around into the Atlantic sector of the Southern Ocean [*Mackensen et al.*, 1993; *Bickert and Wefer*, 1996; *Ninnemann and Charles*, 2002]. The North Pacific was less depleted in δ¹³C at the LGM than the Southern Ocean. The reason for this displacement has been a major mystery. The model shows in very simple terms how it comes about.

[61] Figure 10 compares maps of δ¹³C in the model at a depth of 2430 m. The top panel shows results from the modern time slice; the bottom panel shows results from the glacial slice. The most depleted water in the modern time slice is found in the northeastern corner of the Pacific, as observed, in the water mass most distant from the two sources of ventilated water. Water at 2430 m has two sources of well-ventilated high- δ¹³C deep water, one in the North Atlantic and one in the Southern Ocean.

[62] In the glacial time slice (bottom panel), the deep ocean has only one source of well-ventilated water (the North Atlantic). The most depleted, low- δ¹³C water is found south of the ACC in the Atlantic sector of the Southern Ocean, as seen in the paleo observations. In the absence of a source of ventilated water in the south, the intermediate waters in the North and South Pacific become weak secondary sources for the middle depths of the ocean. These secondary sources become heavier in δ¹³C because the whole upper ocean is heavier in δ¹³C in relation to the deep ocean. The deep water at 2430 m is influenced by these secondary sources. The δ¹³C minimum shifts around to the Atlantic sector of the Southern Ocean because the deep water south of the ACC in the Atlantic becomes the most isolated water mass in the ocean with respect to the North Atlantic and the secondary sources in the Pacific.

5. Discussion

[63] Most recent attempts to address the glacial-interglacial CO₂ problem have been focused on nutrient utilization and biogeochemistry of the Southern Ocean [e.g., *Martin*, 1990; *Watson et al.*, 2000; *Anderson et al.*, 2002; *Bopp et al.*, 2003]. The model here reproduces most of the CO₂ differences between the modern ocean and the glacial ocean through a simple switch in the circulation. The biogeochemistry in the model continues to do what it does in the modern state. The circulation switch operates in response to a change in the wind forcing around Antarctica. The Discussion below revisits past discussions about the glacial-interglacial CO₂ problem and shows how they are reframed by this role for the circulation and the winds.

5.1. Whither the Biological Pump?

[64] *Broecker* [1982] showed that the low pCO₂ of the glacial atmosphere was associated with a larger δ¹³C gradient between the surface ocean and the deep ocean. He drew on the δ¹³C evidence to suggest that the glacial ocean retained more CO₂ because it had more nutrients and more biological productivity, i.e., a stronger "biological pump." Evidence to support a massive increase in biological productivity never materialized, however, and the search for a cause shifted to the Southern Ocean after the publication of the "Harvardton Bears" papers in 1984 [*Sarmiento and Toggweiler*, 1984; *Siegenthaler and Wenk*, 1984; *Knox and McElroy*, 1984].

[65] The current debate about the role of the Southern Ocean is framed around two perspectives on the Harvardton Bears result. One builds on the biological pump idea. The other is built on circulation and gas exchange. A brief synopsis of the two perspectives is given below.

[66] All of the density classes in the deep ocean outcrop at the surface around Antarctica, and the surface waters in these outcrop areas have high concentrations of nitrate and
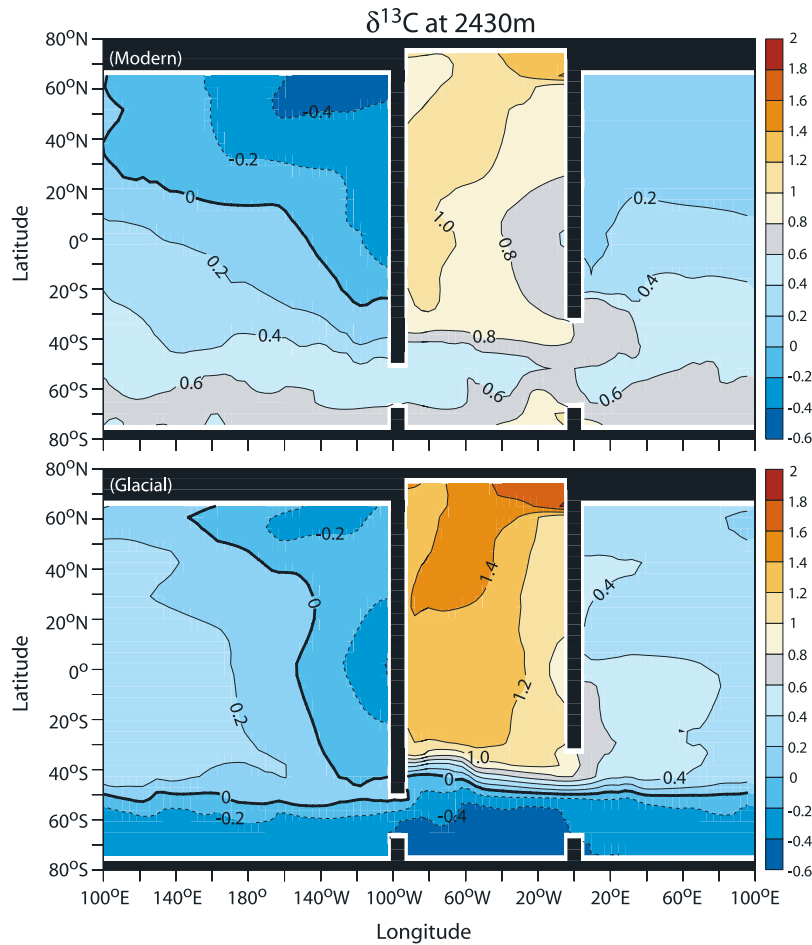
Figure 10. (top) Distribution of δ^{13}C at a depth of 2430 m at the "Modern" time slice in Figure 8. (bottom) The δ^{13}C at the time marked "Glacial" in Figure 8. Units are per mil. The buildup of respired CO$_2$ in southern deep water in Figure 9 causes the ocean's δ^{13}C minimum to shift around from the North Pacific to the Atlantic sector of the Southern Ocean.

phosphate. One interpretation is that this nitrate and phosphate is "unused" or "underutilized" by the phytoplankton. The ocean can retain more respired CO$_2$ if the organisms in the Southern Ocean are more efficient in their use of this underutilized resource. The high-nutrient surface waters of the modern Southern Ocean have a high pCO$_2$ that ultimately sets the pCO$_2$ of the atmosphere. More efficient use of the nutrients by organisms would lower the pCO$_2$, lower the surface nutrients, and cause respired CO$_2$ to build up in the deep ocean.

[67] The other view does not see the nutrients in the Southern Ocean as being "underutilized." High southern nutrient concentrations are instead a manifestation of the upwelling of deep water that takes place along the southern flank of the ACC [*Toggweiler*, 1999; *Stephens and Keeling*, 2000; *Gildor et al.*, 2002]. The atmospheric pCO$_2$ is high during interglacial periods because the circulation brings deep water that is rich in respired CO$_2$ right up to the surface. In this way, most of the respired CO$_2$ in the upwelled deep water is given up to the atmosphere before the upwelled water sinks again [*Toggweiler et al.*, 2003]. Organisms do not have it within their power to utilize more than a small portion of the upwelled nutrients.

[68] The critical distinction between the two perspectives can be narrowed down to the region in the Southern Ocean where this ventilation process occurs. The box models in the Harvardton Bears papers assume that this ventilation process occurs over the entire Southern Ocean. Organisms all over the Southern Ocean get a crack at the nutrients in the upwelled deep water before it can sink again. This is not very realistic.

[69] The other perspective breaks up the Southern Ocean into two domains, one close to Antarctica, and one further out, the subantarctic zone beyond the Polar Front. Biology and nutrient utilization are important only in the subantarctic zone. The switch operates in the upwelling/sinking zone close to Antarctica. Control of atmospheric CO$_2$ belongs to the processes next to Antarctica that govern the amount of

ventilated southern water that sinks back into the deep ocean [*Archer et al.*, 2003; *Toggweiler et al.*, 2003].

5.2. Whither the Westerlies?

[70] Early attempts to locate the glacial westerlies with paleo proxies were equivocal; one school argued for equatorward shifted westerlies [*Heusser*, 1989] and another supported poleward shifted westerlies [*Markgraf*, 1989]. No one in the early 1990s identified the westerlies as a particularly important factor for the global climate.

[71] Observers of the modern atmosphere, meanwhile, began to notice that the mean position of the Southern Hemisphere westerlies has been shifting poleward over the last 40 years [*Hurrell and van Loon*, 1994]. This change in position is reflected in a pattern of month-to-month and year-to-year variability called the Southern Annular Mode (SAM). Model simulations from the mid 1990s hinted that there might be a small intensification and a poleward shift of the westerlies in our greenhouse future [*Kushner et al.*, 2001; *Intergovernmental Panel on Climate Change*, 2001]. Current coupled models produce much more substantial poleward shifts in their greenhouse warming scenario runs [*Yin*, 2005; *Stouffer et al.*, 2006].

[72] The SAM and its northern cousin, the Northern Annular Mode (NAM), are characterized by a seesaw in atmospheric mass between the polar cap regions poleward of 60° latitude and the surrounding zonal rings centered near 45° latitude [*Thompson and Wallace*, 1998, 2001; *Thompson and Solomon*, 2002]. The atmospheric pressure inside the polar caps is low with respect to the pressure at 45° in accord with the strong westerly flow between 45° and 60°. When the pressure difference between the polar cap and the surrounding ring is larger than normal, i.e., when the annular modes are in their "high-index" polarity, the belt of westerly winds is displaced poleward from its climatological mean position. When the pressure difference is smaller than normal, i.e., in the "low-index" state, the westerly belt is displaced toward the equator.

[73] *Hurrell and van Loon* [1994], *Graf et al.* [1995], *Hurrell* [1995], *Thompson et al.* [2000] and *Thompson and Solomon* [2002] have all noted temporal trends in the SAM and NAM toward the high-index state (i.e., more frequent high-index years) over the last 40 years as the climate in both hemispheres has warmed. *Fyfe et al.* [1999] and *Shindell et al.* [1999] have successfully reproduced trends toward a high-index type variability in models that are forced with higher levels of atmospheric CO$_2$.

[74] The poleward shifts in the westerlies over the last 40 years and the evidence tying these shifts to greenhouse warming would suggest that the westerlies also shifted poleward as CO$_2$ increased and the climate warmed at the end of the last ice age. This would imply that the westerlies at the LGM were equatorward of their Holocene position. Indeed, the recent work with paleo proxies supports the idea of a very large equatorward shift at the LGM.

[75] *Moreno et al.* [1999] put the glacial westerlies in South America at around 41°S compared with 50°S today. This result is based on pollen studies that track the migrations of vegetation types found near the tip of South America. The most distinctive is the bog assemblage of the Magellanic Moorlands, which thrives today under the cold and wet conditions within the westerly storm track (48°–56°S). This vegetation type is found at lower latitudes only at high elevations. At the LGM, this vegetation type is found near sea level at 41°S. Moreno et al. conclude that the northern edge of the westerly storm track must have been north of 41°S.

[76] *Lamy et al.* [1999] and *Stuut and Lamy* [2004] have examined the sediments recovered from sites off the coasts of Chile and Namibia. They identify the sediments as wind-blown dust or as fluvial sediment eroded from the continents by rain. Today, these sites receive mainly wind-blown dust from arid environments because they are so far north of the westerly storm track. These same sites received mainly fluvial sediment at the LGM. A Chilean site at 33°S that is located near a coastal desert today received fluvial input from low-elevation coastal range source rocks. This suggests that the westerly storm track at the LGM was close by.

[77] This pattern of wet and dry extends into the Holocene. *Lamy et al.* [2001] and *Lamy et al.* [2002] show that the warm middle Holocene (5000–8000 kyrs B.P.) and the Medieval Warm Period are dry periods in central Chile and times of relative warmth with less sea ice around Antarctica. The cool late Holocene and Little Ice Age are wet periods in central Chile and colder periods with more sea ice around Antarctica. This is further evidence that the westerly storm track moves systematically with the mean climate.

[78] The westerly shifts over the last 40 years can be linked to changes in the upper troposphere that extend up into the stratosphere. *Steinbrecht et al.* [1998], *Thuburn and Craig* [1997] and *Santer et al.* [2003] have shown that the troposphere/stratosphere boundary has been displaced upward as the climate has warmed. This is consistent with the fact that there has been more warming in the upper troposphere than at the surface. The stratosphere, meanwhile, has been cooling in response to higher CO$_2$.

[79] These changes in the upper troposphere indicate that the pocket of warm air near the Earth's surface is not only getting warmer, it is also expanding upward at low latitudes, and the thermal contrast between the pocket of warm air and the surrounding envelope of cold air in the stratosphere is increasing. This means that there is more baroclinicity and a stronger circulation aloft than there was 40 years ago. The poleward shifted, high-index westerlies at the surface are an expression of the stronger circulation aloft [*Thompson and Solomon*, 2002; *Shindell and Schmidt*, 2004; *Yin*, 2005].

[80] *Broecker and Denton* [1989] showed that the snow line on mountain peaks was uniformly lower at the LGM; that is, individual isotherms in the middle of the troposphere were about 1 km lower at the LGM in relation to their positions today. This observation suggests that the pocket of warm air in the troposphere was cool and thin relative to today. It would also suggest that there was less baroclinicity and a weaker circulation aloft, a state that would be consistent with equatorward shifted westerlies at the surface.

5.3. Southern Ocean Stratification and the Role of Sea Ice

[81] Antarctica is surrounded by a layer of relatively fresh surface water that has the potential to isolate the deep water

below from the atmosphere. The stratification associated with the fresh layer is often described as a barrier for CO$_2$ [*Francois et al.*, 1997; *Sigman and Boyle*, 2000; *Gildor et al.*, 2002]. The same can be said of the sea ice at the surface that can limit the exchange of CO$_2$ across the air-sea interface [*Stephens and Keeling*, 2000]. The hypothesis in this paper is that glacial-interglacial CO$_2$ changes take place along with a shift in the westerlies but the stratification and sea ice barriers are also playing a role.

[82] Stratification in the polar oceans is enhanced by colder temperatures [*Sigman et al.*, 2004]. Thus a cool climate perturbation that lowers atmospheric CO$_2$ by increasing CO$_2$ solubility would also strengthen the stratification around Antarctica and cause the ice pack to expand and thicken. The cooling effect on the barriers could then cause respired CO$_2$ to build up in the deep ocean, which would lead to an even greater reduction in CO$_2$. Perhaps the barriers are capable of lowering atmospheric CO$_2$ through a feedback of their own. Is a wind shift really necessary?

[83] A windless feedback may not be big enough to get the ball rolling. The modern Ekman transport draws up warm salty deep water from below to replace the fresh surface waters that are continuously carried away to the north [*Gordon*, 1971]. The warm upwelled water also melts the ice at the surface and keeps the ice pack fairly thin. A cool perturbation that does not shift the westerlies has to overcome these effects. Hence a more likely scenario is that the barriers work together with the westerlies to produce a stronger feedback. A cool perturbation that shifts the westerlies equatorward reduces the upwelling from below and makes it easier for the stratification and a thicker ice pack to develop.

[84] *Adkins et al.* [2002] recovered ancient pore water from Southern Ocean sediments, which shows that the bottom water of the glacial Southern Ocean was the saltiest water in the deep ocean at that time. They suggested that the salty deep water was produced from the brine rejected by an expanded glacial ice pack. These findings support the idea that thick ice was a factor in the low CO$_2$ at the LGM [*Stephens and Keeling*, 2000]. They do not tell us how and when the ice buildup came about.

[85] *Stouffer and Manabe* [2003] reproduced the *Adkins et al.* [2002] result in a coupled model that was run with half the preindustrial level of atmospheric CO$_2$. The low CO$_2$ imposed in the model leads to the production of thick sea ice, which drives a strong circulation in the salty bottom waters. The abyssal circulation in the Stouffer and Manabe model develops after the low CO$_2$ is imposed and the model climate becomes very cold.

[86] The Adkins et al. and Stouffer and Manabe results are not part of the model solutions generated here, but they are not inconsistent. Adkins et al.'s salty bottom water was apparently very depleted in δ^{13}C (Figures 1 and 2). This means that the salty bottom water had no contact with the atmosphere. A vigorous deep circulation that is initiated under thick sea ice and is not in contact with the atmosphere is the same as a dead blue circulation in the present context. Unless it can be shown that the salty bottom water developed before the atmospheric pCO$_2$ came down, we will

assume that Adkins et al.'s salty bottom water is a feature that developed during the cold state.

5.4. Temporal Setting for the Feedback

[87] The δ^{13}C observations from *Hodell et al.* [2003] in Figure 2 show that the deep ocean accumulates respired CO$_2$ over a short period of time at the beginning of each glacial period and then abruptly loses all of this CO$_2$ at the beginning of the next interglacial. It tends to stay in the same state from one transition to the next. The intervals between these transitions seem to be fairly regular. Respired CO$_2$ accumulated at 70,000, 180,000, 370,000, and 460,000 years ago, i.e., about every 100,000 years. It was vented away at 15,000, 120,000, 320,000, and 410,000 years ago, about 50,000 years after the preceding accumulation event.

[88] This pattern is similar to the pattern in the CO$_2$ time series from the Vostok ice core [*Petit et al.*, 1999] in the sense that the atmosphere is also spending most of its time with a pCO$_2$ that is close to one of its extremes. The atmospheric pCO$_2$ resides in an average state only briefly while it is transitioning from one extreme to the other.

[89] The CO$_2$ time series from the Vostok ice core extends back 420,000 years. This is long enough that the mean pCO$_2$ of the time series, roughly 230 ppm, should reflect the long-term steady state pCO$_2$ that is maintained by volcanoes and weathering. This makes the behavior of atmospheric CO$_2$ over the last half million years seem particularly odd: despite the fact that volcanoes and weathering are pulling the atmospheric pCO$_2$ back to a long-term mean state between the glacial and interglacial extremes, the system seems to be going out of its way to avoid ever being in the mean state.

[90] Why does the CO$_2$ system exhibit this behavior? Why are the deep ocean and atmosphere avoiding their mean states, and why do they flip to the opposite state with the particular timescale seen in Figure 2? We interpret these transitions as evidence for a threshold in the climate system.

[91] A long-term steady state pCO$_2$ of ~230 ppm corresponds to an intermediate temperature for the Earth that is also between the glacial and interglacial extremes. This intermediate temperature should, in turn, correspond to an intermediate position or an intermediate intensity of the Southern Hemisphere westerlies. Figure 11 shows a schematic diagram of the South Pacific with the position of the ACC and the approximate positions of the glacial and interglacial westerlies sketched in. The axis of the modern westerlies is shown overlying the ACC, while the axis of the glacial westerlies is far to the north. The long-term mean position of the westerlies is presumed to be somewhere in the middle between the modern and glacial limits.

[92] We imagine that the westerlies have been sweeping back and forth between these limits in accord with the CO$_2$ and temperature variations of the last 500,000 years. The feedback pushes the westerlies to the southern limit in a warming climate and it pushes the westerlies to the northern limit in a cooling climate. This implies that the intermediate position in between is unstable with respect to the feedback. The intermediate position is therefore a threshold in the CO$_2$/climate system.
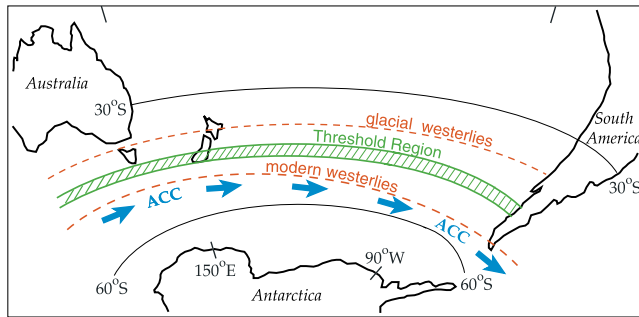
Figure 11. Schematic diagram showing the position of the strongest westerlies today and the strongest westerlies at the Last Glacial Maximum in relation to the position of the Antarctic Circumpolar Current (ACC). The westerlies are pushed to these limits by the positive feedback described in the text. The intermediate position between these limits is assumed to be unstable with respect to the feedback and is therefore a threshold in the CO$_2$/climate system. The threshold and the north-south limits on the westerlies extend into the Indian and Atlantic.

[93] The threshold is depicted as the green hatched region in Figure 11, i.e., as a position on a map. It could also be a critical wind intensity, like the 1.5x wind forcing in the model. The important thing is that the threshold, whatever it is, occupies an intermediate position between the extremes that mirrors the intermediate position/intensity of the westerlies favored by the long-term mean pCO$_2$.

[94] The overarching idea behind this paper and the one to follow is that the CO$_2$ cycles and big ice ages of the last 500,000 years owe their existence to this overlap: The position of the westerlies favored by the long-term steady state pCO$_2$ overlies the position where the feedback has its threshold. This kind of overlap could explain the peculiar cyclic behavior seen in Figure 2 and in the Vostok CO$_2$ record: the feedback is always driving the westerlies and the pCO$_2$ away from the intermediate position occupied by the threshold while the Earth's volcanoes and weathering are always trying to bring them back. Once they fall back to the intermediate position, the next feedback event sends them off to the opposite extreme.

[95] The feedback described here can only push the westerlies and the pCO$_2$ *away* from the threshold. It is also bounded by the fact that the ocean can hold and give up only so much respired CO$_2$. Hence the feedback is expended once the westerlies reach the southern and northern limits in Figure 11. At this point the feedback is powerless to stop the westerlies and the pCO$_2$ from falling back from their extreme positions. The deep ocean, meanwhile, is set up to flip the other way. When the westerlies and pCO$_2$ reach the threshold again, the feedback goes off in the other direction.

[96] Astute readers will have noted that the 50,000-year period between the accumulation and venting events in Figure 2 is much shorter than the 400,000-year timescale for volcanism and weathering to bring the pCO$_2$ back to the long-term mean [*Walker et al.*, 1981; *Marty and Tolstikhin*,

1998]. We will show in the follow-up paper that 50,000 years is an intrinsic timescale for the ocean's chemistry to adjust to the accumulation or venting of respired CO$_2$. The pCO$_2$ of the atmosphere tends to be "held away" from the threshold during this adjustment period. As such, the glacial and interglacial climates are "protected" from short-term perturbations like those seen during the last glacial period [*Indermuhle et al.*, 2000; *Blunier and Brook*, 2001].

[97] After the ocean's chemical adjustment has run its course, this protection is over and the next perturbation to come along (with the right sign) can bring the pCO$_2$ back to the threshold and set off the next feedback event. Thus volcanoes and weathering do not actually bring the pCO$_2$ back to the threshold. They keep the long-term steady state pCO$_2$ centered over the threshold so that random perturbations (of the appropriate sign) can bring the pCO$_2$ back after the adjustment period. Two of these adjustments and two fast transitions add up to 100,000 years, the dominant period of variability in the Vostok CO$_2$ record [*Petit et al.*, 1999].

[98] The overlap between the position of the westerlies favored by the long-term mean pCO$_2$ and the threshold is a coincidence, we would argue, that developed about 500,000 years ago when a slow decline in the volcanic output of CO$_2$ brought the Earth's mean temperature and the mean position of the westerlies into alignment with the threshold. Before this time, the Earth was too warm and the westerlies were too strong or too far poleward. The earliest cycle presumably began about a million years ago when a lower pCO$_2$ first brought the westerlies and the Earth's temperatures within range of the threshold. The cycles then became larger and more regular as the mean position of the westerlies came to overlie the threshold.

6. Conclusions

[99] This paper introduces several new concepts. The first is the positive feedback described in section 3 that drives the CO$_2$/climate system to its glacial and interglacial extremes. The second is the idea of a threshold in the CO$_2$/climate system where the feedback changes sign or direction. The CO$_2$ and ice age cycles of the last half million years owe their existence, we claim, to the fact that the long-term mean pCO$_2$ set by volcanoes and weathering overlaps with this threshold. This arrangement guarantees that the feedback will continue to be triggered time after time.

[100] The key process is the ventilation of the deep Southern Ocean and its relationship to the westerly winds in the atmosphere. Strong westerlies over the ACC bring deep water laden with respired CO$_2$ directly up to the surface where the respired CO$_2$ is rather easily vented to the atmosphere. Westerlies shifted away from the ACC shut down this process by allowing a low-salinity cap and thick sea ice to develop over the Southern Ocean. The westerlies over the Southern Ocean seem to be stronger and/or poleward shifted in warm climates and weaker and/or equatorward shifted in cool climates. This tendency turns the Southern Ocean's wind/ventilation relationship into a positive feedback. Atmospheric CO$_2$ and Antarctic temperatures rise and fall together as part of the feedback.

[101] The idealized model in this paper has an internal threshold and a switch-like behavior that simulates the rise of atmospheric CO$_2$ along with Antarctic temperatures at glacial terminations. A slight CO$_2$ lag behind the rise in Antarctic temperatures is an intrinsic feature as is the shift of the ocean's δ^{13}C minimum from the Atlantic sector of the Southern Ocean around to the North Pacific. The threshold in the model is not the same as the threshold/ feedback effect hypothesized for the real world, however. The full effect requires interactions that the present model does not have.

[102] A key prediction for the real world is that the intermediate climate state between the glacial and interglacial extremes is unstable. A cool climate with a pCO$_2$ of ∼230 ppm should spontaneously give way, via the feedback, to a climate state that is more like one extreme or the other.

References

Adkins, J. F., K. McIntyre, and D. P. Schrag (2002), The salinity, temperature, and δ^{18}O of the glacial deep ocean, *Science*, *298*, 1769–1773.

Anderson, R. F., Z. Chase, M. Q. Fleisher, and J. Sachs (2002), The Southern Ocean's biological pump during the Last Glacial Maximum, *Deep Sea Res., Part II*, *49*, 1909–1938.

Archer, D. E., P. A. Martin, J. Milovich, V. Brovkin, G. Plattner, and C. Ashendel (2003), Model sensitivity in the effect of Antarctic sea ice and stratification on atmospheric pCO$_2$, *Paleoceanography*, *18*(1), 1012, doi:10.1029/2002PA000760.

Bickert, T., and G. Wefer (1996), Late Quaternary deep water circulation in the South Atlantic: Reconstruction from carbonate dissolution and benthic stable isotopes, in *The South Atlantic: Present and Past Circulation*, edited by G. Wefer et al., pp. 599–620, Springer, New York.

Blunier, T., and E. J. Brook (2001), Timing of millennial-scale climate change in Antarctica and Greenland during the last glacial period, *Science*, *291*, 109–112.

Bopp, L., K. E. Kohfeld, C. LeQuere, and O. Aumont (2003), Dust impact on marine biota and atmospheric CO$_2$ during glacial periods, *Paleoceanography*, *18*(2), 1046, doi:10.1029/2002PA000810.

Boyle, E. A. (1988), The role of vertical chemical fractionation in controlling late Quaternary atmospheric carbon dioxide, *J. Geophys. Res.*, *93*, 15,701–15,714.

Boyle, E. A. (1992), Cadmium and δ^{13}C paleochemical ocean distributions during the stage 2 glacial maximum, *Annu. Rev. Earth. Planet. Sci.*, *20*, 245–287.

Broecker, W. S. (1982), Glacial to interglacial changes in ocean chemistry, *Prog. Oceanogr.*, *11*, 151–197.

Broecker, W. S., and G. H. Denton (1989), The role of ocean-atmosphere reorganizations in glacial cycles, *Geochim. Cosmochim. Acta*, *53*, 2465–2501.

Broecker, W. S., and T.-H. Peng (1987), The role of CaCO$_3$ compensation in the glacial to interglacial atmospheric CO$_2$ change, *Global Biogeochem. Cycles*, *1*, 15–29.

Bryan, K., and L. Lewis (1979), A water mass model of the World Ocean, *J. Geophys. Res.*, *84*, 2503–2517.

Caillon, N., J. P. Severinghaus, J. Jouzel, J.-M. Barnola, J. Kang, and V. Y. Lipenkov (2003), Timing of atmospheric CO$_2$ and Antarctic temperature changes across Termination III, *Science*, *299*, 1728–1731.

Cuffey, K. M., and F. Vimeux (2001), Covariation of carbon dioxide and temperature from the Vostok ice core after deuterium-excess correction, *Nature*, *412*, 523–527.

Curry, W. B., J. C. Duplessy, L. D. Labeyrie, and N. J. Shackleton (1988), Quaternary deepwater circulation changes in the distribution of δ^{13}C of deep water $\sum$CO$_2$ between the last glaciation and the Holocene, *Paleoceanography*, *3*, 317–342.

Delmas, R. J., J.-M. Ascencio, and M. Legrand (1980), Polar ice evidence that atmospheric CO$_2$ 20,000 yr BP was 50% of present, *Nature*, *284*, 155–157.

Duplessey, J.-C., N. J. Shackleton, R. G. Fairbanks, L. Labeyrie, D. Oppo, and N. Kallel (1988), Deepwater source variations during the last climatic cycle and their impact on the global deep water circulation, *Paleoceanography*, *3*, 343–360.

Fischer, H., M. Wahlen, J. Smith, D. Mastroianni, and B. Deck (1999), Ice core records of atmospheric CO$_2$ around the last three glacial terminations, *Science*, *283*, 1712–1714.

Flower, B. P., D. W. Oppo, J. F. McManus, K. A. Venz, D. A. Hodell, and J. L. Cullen (2000), North Atlantic intermediate to deep water circulation and chemical stratification during the past 1 Myr, *Paleoceanography*, *15*, 388–403.

Foster, T. D., and E. C. Carmack (1976), Frontal zone mixing and Antarctic Bottom Water formation in the southern Weddell Sea, *Deep Sea Res. Oceanogr. Abstr.*, *23*, 301–317.

Francois, R. F., et al. (1997), Water column stratification in the Southern Ocean contributed to the lowering of glacial atmospheric CO$_2$, *Nature*, *389*, 929–935.

Fyfe, J. C., G. J. Boer, and G. M. Flato (1999), The Arctic and Antarctic Oscillations and their projected changes under global warming, *Geophys. Res. Lett.*, *26*, 1601–1604.

Gildor, H., E. Tziperman, and J. R. Toggweiler (2002), Sea ice switch mechanism and glacial-interglacial CO$_2$ variations, *Global Biogeochem. Cycles*, *16*(3), 1032, doi:10.1029/2001GB001446.

Gnanadesikan, A. (1999), A simple predictive model for the structure of the oceanic pycnocline, *Science*, *283*, 2077–2079.

Gordon, A. (1971), Oceanography of Antarctic waters, in *Antarctic Oceanology I, Antarct.* *Res. Ser.*, vol. 15, edited by J. L. Reid, pp. 169–203, AGU, Washington, D. C.

Graf, H.-F., J. Perlwitz, I. Kirchner, and I. Schult (1995), Recent northern winter climate trends, ozone changes and increased greenhouse forcing, *Contrib. Atmos. Phys.*, *68*, 233–248.

Griffies, S. M. (1998), The Gent-McWilliams skew flux, *J. Phys. Oceanogr.*, *28*, 831–841.

Hellerman, S., and M. Rosenstein (1983), Normal monthly wind stress over the world ocean with error estimates, *J. Phys. Oceanogr.*, *13*, 1093–1104.

Herguera, J. C., E. Jansen, and W. H. Berger (1992), Evidence for a bathyal front at 2000 m depth in the glacial Pacific, based on a depth transect on the Ontong Java Plateau, *Paleoceanography*, *7*, 273–288.

Heusser, C. J. (1989), Southern westerlies during the Last Glacial Maximum, *Quat. Res.*, *31*, 423–425.

Hodell, D. A., K. A. Venz, C. D. Charles, and U. S. Ninnemann (2003), Pleistocene vertical carbon isotope and carbonate gradients in the South Atlantic sector of the Southern Ocean, *Geochem. Geophys. Geosyst.*, *4*(1), 1004, doi:10.1029/2002GC000367.

Hurrell, J. W. (1995), Decadal trends in the North Atlantic Oscillation: Regional temperatures and precipitation, *Science*, *269*, 676–679.

Hurrell, J. W., and H. van Loon (1994), A modulation of the atmospheric annual cycle in the Southern Hemisphere, *Tellus, Ser. A*, *46*, 325–338.

Indermuhle, A., E. Monnin, B. Stauffer, and T. F. Stocker (2000), Atmospheric CO$_2$ concentration from 60–20 kyr BP from the Taylor Dome ice core, Antarctica, *Geophys. Res. Lett.*, *27*, 735–738.

Intergovernmental Panel on Climate Change (2001), *Climate Change 2001: The Scientific Basis: Contributions of Working Group 1 to the Third Assessment Report of the Intergovernmental Panel on Climate Change*, edited by J. T. Houghton et al., 881 pp., Cambridge Univ. Press, New York.

Knox, F., and M. B. McElroy (1984), Changes in atmospheric CO$_2$: Influence of the marine biota at high latitude, *J. Geophys. Res.*, *89*, 4629–4637.

Knutson, T. R., and S. Manabe (1998), Model assessment of decadal variability and trends in the tropical Pacific Ocean, *J. Clim.*, *11*, 2273–2296.

Kroopnick, P. (1985), The distribution of ^{13}C and $\sum$CO$_2$ in the world oceans, *Deep Sea Res., Part A, 32*, 57–84.

Kushner, P. J., I. M. Held, and T. L. Delworth (2001), Southern Hemisphere atmospheric circulation response to global warming, *J. Clim., 14*, 2238–2249.

Lamy, F., D. Hebbeln, and G. Wefer (1999), High-resolution marine record of climatic change in mid-latitude Chile during the last 28,000 years based on terrigenous sediment parameters, *Quat. Res., 51*, 83–93.

Lamy, F., D. Hebbeln, U. Rohl, and G. Wefer (2001), Holocene rainfall variability in southern Chile: A marine record of latitudinal shifts of the southern westerlies, *Earth Planet. Sci. Lett., 185*, 369–382.

Lamy, F., C. Ruhlemann, D. Hebbeln, and G. Wefer (2002), High- and low-latitude climate control on the position of the southern Peru-Chile Current during the Holocene, *Paleoceanography, 17*(2), 1028, doi:10.1029/2001PA000727.

Mackensen, A., H.-W. Hubberten, T. Bickert, G. Fischer, and D. K. Fütterer (1993), The δ^{13}C of benthic foraminiferal tests of Fontboita wuellerstorfi (Schwager) relative to the δ^{13}C of dissolved inorganic carbon in Southern Ocean deep water: Implications for glacial ocean circulation models, *Paleoceanography, 8*, 587–610.

Mackensen, A., M. Rudolph, and G. Kuhn (2001), Late Pleistocene deep-water circulation in the subantarctic eastern Atlantic, *Global Planet. Change, 30*, 197–229.

Markgraf, V. (1989), Reply to Heuser's "Southern westerlies during the Last Glacial Maximum," *Quat. Res., 31*, 426–432.

Martin, J. H. (1990), Glacial-interglacial CO$_2$ changes: The iron hypothesis, *Paleoceanography, 5*, 1–13.

Marty, B., and I. N. Tolstikhin (1998), CO$_2$ fluxes from mid-ocean ridges, arcs, and plumes, *Chem. Geol., 145*, 233–248.

Matsumoto, K., and J. Lynch-Stieglitz (1999), Similar glacial and Holocene deep water circulation inferred from southeast Pacific benthic foraminiferal carbon isotope composition, *Paleoceanography, 14*, 149–163.

Milankovitch, M. (1930), *Mathematische Klimalehre und Astronomische Theorie der Klimaschwankungen*, 176 pp., Gebrüder Borntraeger, Stuttgart, Germany.

Moreno, P. I., T. V. Lowell, G. L. Jacobson Jr., and G. H. Denton (1999), Abrupt vegetation and climate changes during the Last Glacial Maximum and last termination in the Chilean Lake District: A case study from Canal de la Puntilla (41°S), *Geogr. Ann., Ser. A, 81*, 285–311.

Neftel, A., H. Oeschger, J. Schwander, B. Stauffer, and R. Zumbrunn (1982), Ice core sample measurements give atmospheric CO$_2$ content during the past 40,000 yr, *Nature, 295*, 220–223.

Ninnemann, U. S., and C. D. Charles (2002), Changes in the mode of Southern Ocean circulation over the last glacial cycle revealed by foraminiferal stable isotopic variability, *Earth Planet. Sci. Lett., 201*, 383–396.

Petit, J. R., et al. (1999), Climate and atmospheric history of the past 420,000 years from the Vostok ice core, Antarctica, *Nature, 399*, 429–436.

Santer, B. D., et al. (2003), Behavior of tropopause height and atmospheric temperature in models, reanalyses, and observations: Decadal changes, *J. Geophys. Res., 108*(D1), 4002, doi:10.1029/2002JD002258.

Sarmiento, J. L., and J. R. Toggweiler (1984), A new model for the role of the oceans in determining atmospheric CO$_2$, *Nature, 308*, 621–624.

Sarnthein, M., K. Winn, S. J. A. Jung, J. Duplessy, L. Labeyrie, H. Erlenkeuser, and G. Ganssen (1994), Changes in east Atlantic deepwater circulation over the last 30,000 years: Eight time slice reconstructions, *Paleoceanography, 9*, 209–267.

Shackleton, N. J. (2000), The 100,000-year ice-age cycle identified and found to lag temperature, carbon dioxide, and orbital eccentricity, *Science, 289*, 1897–1902.

Shackleton, N. J., and N. G. Pisias (1985), Atmospheric carbon dioxide, orbital forcing, and climate, in *The Carbon Cycle and Atmospheric CO$_2$: Natural Variations Archean to Present, Geophys. Monogr. Ser.*, vol. 32, edited by E. T. Sundquist, and W. S. Broecker, pp. 303–317, AGU, Washington, D. C.

Shindell, D. T., and G. A. Schmidt (2004), Southern Hemisphere climate response to ozone changes and greenhouse gas increases, *Geophys. Res. Lett., 31*, L18209, doi:10.1029/2004GL020724.

Shindell, D. T., R. L. Miller, G. A. Schmidt, and L. Pandolfo (1999), Simulation of recent northern winter climate trends by greenhouse-gas forcing, *Nature, 399*, 452–455.

Siegenthaler, U., and T. Wenk (1984), Rapid atmospheric CO$_2$ variations and ocean circulation, *Nature, 308*, 624–626.

Sigman, D. M., and E. A. Boyle (2000), Glacial/interglacial variations in atmospheric carbon dioxide, *Nature, 407*, 859–869.

Sigman, D. M., S. L. Jaccard, and G. H. Haug (2004), Polar ocean stratification in a cold climate, *Nature, 428*, 59–63.

Sowers, T., M. Bender, D. Raynaud, Y. S. Korotkevich, and J. Orchardo (1991), The δ^{18}O of atmospheric O$_2$ from air inclusions in the Vostok ice core: Timing of CO$_2$ and ice volume changes during the penultimate deglaciation, *Paleoceanography, 6*, 679–696.

Steinbrecht, W., H. Claude, and U. Kohler (1998), Correlations between tropopause height and total ozone: Implications for long-term changes, *J. Geophys. Res., 103*, 19,183–19,192.

Stephens, B. B., and R. F. Keeling (2000), The influence of Antarctic sea ice on glacial-interglacial CO$_2$ variations, *Nature, 404*, 171–174.

Stouffer, R., and S. Manabe (2003), Equilibrium response of thermohaline circulation to large changes in atmospheric CO$_2$ concentrations, *Clim. Dyn., 20*, 759–773.

Stouffer, R. J., et al. (2006), GFDL's CM2 global coupled models–part 4: Idealized climate response, *J. Clim., 19*, 723–740.

Stuut, J.-B. W., and F. Lamy (2004), Climate variability at the southern boundaries of the Namib (southwestern Africa) and Atacama (northern Chile) coastal deserts during the last 120,000 years, *Quat. Res., 62*, 301–309.

Thompson, D. W. J., and S. Solomon (2002), Interpretation of recent Southern Hemisphere climate change, *Science, 296*, 895–899.

Thompson, D. W. J., and J. M. Wallace (1998), The Arctic Oscillation signature in the wintertime geopotential height and temperature fields, *Geophys. Res. Lett., 25*, 1297–1300.

Thompson, D. W. J., and J. M. Wallace (2001), Regional climate impacts of the Northern Hemisphere Annular Mode, *Science, 293*, 85–89.

Thompson, D. W. J., J. M. Wallace, and G. C. Hegerl (2000), Annular modes in the extratropical circulation. part II: Trends, *J. Clim., 13*, 1018–1036.

Thuburn, J., and G. C. Craig (1997), GCM tests of theories for the height of the tropopause, *J. Atmos. Sci., 54*, 869–882.

Toggweiler, J. R. (1999), Variation of atmospheric CO$_2$ by ventilation of the ocean's deepest water, *Paleoceanography, 14*, 571–588.

Toggweiler, J. R., and H. Bjornsson (2000), Drake Passage and paleoclimate, *J. Quat. Sci., 15*(4), 319–328.

Toggweiler, J. R., and B. Samuels (1993), New radiocarbon constraints on the upwelling of abyssal water to the ocean's surface, in *The Global Carbon Cycle*, edited by M. Heimann, NATO ASI Ser., Ser. I, vol. 15, pp. 333–366, Springer, New York.

Toggweiler, J. R., and B. Samuels (1995), Effect of Drake Passage on the global thermohaline circulation, *Deep Sea Res., Part I, 42*, 477–500.

Toggweiler, J. R., R. Murnane, S. Carson, A. Gnanadesikan, and J. L. Sarmiento (2003), Representation of the carbon cycle in box models and GCMs: 2. Organic pump, *Global Biogeochem. Cycles, 17*(1), 1027, doi:10.1029/2001GB001841.

Walker, J. C. G., P. B. Hays, and J. F. Kasting (1981), A negative feedback mechanism for the long-term stabilization of Earth's surface temperature, *J. Geophys. Res., 86*, 9776–9782.

Watson, A. J., D. C. E. Bakker, A. J. Ridgwell, P. W. Boyd, and C. S. Law (2000), Effect of iron supply on Southern Ocean CO$_2$ uptake and implications for glacial atmospheric CO$_2$, *Nature, 407*, 730–733.

Weaver, A. J., and E. S. Sarachik (1991), The role of mixed boundary conditions in numerical models of the ocean's climate, *J. Phys. Oceanogr., 21*, 1470–1493.

Weiss, R. F., H. G. Ostlund, and H. Craig (1979), Geochemical studies of the Weddell Sea, *Deep Sea Res., Part A, 26*, 1093–1120.

Williams, G. P., and K. Bryan (2006), Ice age winds: An aquaplanet model, *J. Clim., 19*, 1706–1715.

Wyrtki, K. (1961), The thermohaline circulation in relation to the general circulation in the oceans, *Deep Sea Res., 8*, 39–64.

Yin, J. H. (2005), A consistent poleward shift of the storm tracks in simulations of 21st century climate, *Geophys. Res. Lett., 32*, L18701, doi:10.1029/2005GL023684.

————————————

S. R. Carson, John Witherspoon Middle School, 217 Walnut Street, Princeton, NJ 08540, USA. (steve_carson@monet.prs.k12.nj.us)

J. L. Russell, Department of Geosciences, University of Arizona, Gould-Simpson Building 309, 1040 E. 4th Street, Tuczon, AZ 85721, USA. (jrussell@geo.arizona.edu)

J. R. Toggweiler, Geophysical Fluid Dynamics Laboratory, National Oceanic and Atmospheric Administration, P.O. Box 308, Princeton, NJ 08542, USA. (robbie.toggweiler@noaa.gov)